 DOI: 10.31276/VJSTE.65(3).44-49

Pencil lead graphite electrochemically modified with polyglutamic acid as a sensor for detection of enrofloxacin in aqueous media

Thi Hai Yen Pham[1*], Thi Kim Ngan Nguyen[2, 3], Thi Thu Hien Chu[4], Thi Thu Ha Vu[1], Quoc Hung Le[1]

[1]Institute of Chemistry, Vietnam Academy of Science and Technology, 18 Hoang Quoc Viet Street, Nghia Do Ward, Cau Giay District, Hanoi, Vietnam
[2]Graduate University of Science and Technology, Vietnam Academy of Science and Technology, 18 Hoang Quoc Viet Street, Nghia Do Ward, Cau Giay District, Hanoi, Vietnam
[3]Faculty of Chemistry, University of Sciences, Thai Nguyen University, Tan Thinh Ward, Thai Nguyen City, Thai Nguyen Province, Vietnam
[4]Department of Chemistry, Faculty of Building Materials, Hanoi University of Civil Engineering, 55 Giai Phong Street, Dong Tam Ward, Hai Ba Trung District, Hanoi, Vietnam

Received 13 December 2022; revised 1 March 2023; accepted 6 March 2023

Abstract:

This study investigates the modification of pencil lead graphite electrodes with polyglutamic acid using an effective and fast static method to develop a sensor for the detection of enrofloxacin (ENR). The successful fabrication of pGA on the electrode surface was confirmed by scanning electron microscopy, energy dispersive X-ray analysis, and Fourier-transform infrared spectroscopy. The conditions of electrochemical modification, including the applied potentials and number of cycles in the potentiostatic process, were systematically investigated to determine their effects on the ENR electrochemical response. The pH of the electrolyte media was also explored to elucidate the electrochemical reaction mechanism of ENR. The developed electrochemical sensor was evaluated using square wave stripping voltammetry for ENR detection. Under optimal conditions, the sensor demonstrated good reproducibility with a relative standard deviation of 4.3% (from five measurements) for ENR signal detection. A linear relationship between ENR concentration and its peak current was observed in the concentration range of 0.1 to 5 µM, with a high correlation coefficient of 0.9988. The limit of detection for ENR using the sensor was 0.12 µM. Our findings provide valuable insights into the design and optimisation of pencil lead graphite electrode-based sensors for ENR detection in aqueous media.

Keywords: **electrochemical analysis, electrochemical polymerisation, enrofloxacin detection, glutamic acid, potentiostatic method.**

Classification numbers: **2.2, 5.3**

1. Introduction

ENR has been one of the most widely used antimicrobial drugs for the treatment of infections originating from both gram-positive and gram-negative bacteria in animals [1-3]. The diseases caused by these bacteria include respiratory, mammary, digestive, and dermal infections in livestock and aquaculture [4, 5]. ENR has also been used in the treatment of osteomyelitis, otitis, peritonitis, and pneumonia in humans [6, 7]. Although it has a vital role in preventing humans from microbial infection, the overuse of ENR and its residue can place human health at risk [8, 9]. Besides, the ENR residue generated from human and animal digestion, ENR residues in wastewater is considered a potential risk to the environment due to its accumulation in water and soil [10, 11]. Moreover, antibiotics are considered a factor in the development of anti-bacterial resistant bacteria [12]. Due to these potential dangers, it is crucial to construct analytical methods for the determination of ENR at low concentration ranges in an aqueous environment.

Over past few decades, methods for quantifying ENR have been developed including capillary electrophoresis, high-performance liquid chromatography, liquid chromatography-mass spectrometry, and fluorescence detection [13-17]. These methods provide high accuracy and good sensitivity; however, drawbacks such as extended sample pre-treatment time, complicated operation, requirements for well-trained operators, and high-cost equipment restrict their analytical performance. In recent years, electrochemical determination of ENR has emerged as an effective method owing to advantages like high sensitivity, good selectivity, and convenience [18]. In this method, scientists have mainly focused on modifying the working electrode to improve the electrochemical signal of the target. The modification consists of using nanomaterials like metal nanoparticles, carbon nanomaterials, polymers, organic materials, and metal-organic frameworks [19-25]. These materials have unique properties such as large active surface area, electrochemical catalytic ability, fast electron

*Corresponding author: Email: haiyen25986@gmail.com

transfer, and customised functional groups, making them beneficial for adsorption and electrochemical reactions of analytes on the electrode surface. Recently, polyglutamic acid (pGA) - a completely biodegradable and non-toxic compound - has attracted much attention in electrochemical research applications because its chain contains a series of free protonated carboxyl groups that facilitate interaction and linkages with desirable targets. In addition, pGA is easily produced on a conductive substrate via an electrochemical process with variable sizes of pGA molecules, making it a promising material in electrochemical applications [26-29].

In this study, we present a new method to modify pencil lead with pGA via a potentiostatic technique that has been employed in the detection of ENR for the first time. The fabrication conditions of the developed electrode were investigated to obtain the most effective sensor for ENR detection. This technique was carried out on a cost-effective electrode substrate with faster and simpler preparation methods compared to previously published ones. Besides, the pGA-based sensor, in combination with an eco-friendly environmental modifier, showed good performance in the quantification of ENR.

2. Materials and methods

2.1. Reagents and apparatus

Pencil lead (diameter of 0.5 mm, length of 15 mm) was purchased from Dong-a Pencil Co., Ltd., Korea. L-GA (99%), potassium ferricyanide (99.9%), potassium dihydrogen phosphate (99.9%), and di-potassium hydrogen phosphate (99.9%), were purchased from Merck, Sigma-Aldrich. ENR (98%) was purchased from Tokyo Chemical Industry Co., Ltd., Japan. All reagents were directly used without further purification.

Electrochemical measurements were performed using a home-made multi-functional potentiogalvanostat manufactured at the Institute of Chemistry, Vietnam Academy of Science and Technology, Hanoi, Vietnam. The electrochemical cell contains a three-electrode system consisting of an Ag/AgCl electrode (reference electrode), a platinum wire (auxiliary electrode), and pencil lead (working electrode).

Cyclic voltammetry was used for the investigation of the modified electrode's properties.

Field emission scanning electron microscopy (FE-SEM) (Hitachi S-4800, Japan) and attenuated total reflectance -Fourier transform infrared spectroscopy (ATR-FTIR) (Perkin Elmer, L1600400 Spectrum Two, UK) was used to characterise the morphology of the electrode surface.

2.2. Preparation of modified electrode

Initially, pencil lead electrodes were polished with tissue paper and rinsed with 90% ethanol and double-distilled water. The electrochemical modification of pGA on the pencil lead electrodes was carried out by using a potentiostatic technique in a 0.1-M phosphate buffer solution (PBS) at pH 7 containing 5.0 g of l-1 glutamic acid (GA). In this step, negative and positive potentials were alternatively applied for 10 s for various numbers of cycles. Both synthesis parameters were examined.

2.3. Characterisation of pGA/PLE

Cyclic voltammetry (CV) was used to study the electrochemical property of GA and the modified electrodes. The measurement was performed in 5.0×10^{-3} M $K_3Fe(CN)_6$/0.1 M PBS solution (pH 7) at various scan rates from 10 mV to 100 mV.

The electrode performance in ENR was conducted by using square wave stripping voltammetry (SW-AdSV) in a PBS solution containing ENR at various concentrations.

All experiments were performed at 25±2°C.

3. Results and discussion

3.1. Electrochemical polymerisation of GA on pencil lead electrode

The electrochemical reaction of GA on pencil lead was characterised by cyclic voltammetry to determine suitable voltametric parameters for the polymerisation of GA. Fig. 1A shows cyclic voltammograms of a pencil lead electrode in PBS solution (pH 7) with and without GA. Obviously, no peak was obtained in the free glutamic solution in the examined potential range. Meanwhile, two peaks at -1 and 1.8 V clearly appeared in the GA solution. These peaks correspond to the electrochemical polymerisation of GA on the electrode surface [30, 31]. Hence, suitable potentials for electrode fabrication were selected in the range from -1.2 to 2.0 V.

To synthesise pGA on the pencil lead, a clean pencil lead bar was immersed in GA solution, then the potentiostatic technique was performed in two successive steps. In step 1, a negative potential was applied to the electrode for 10 s to form −COO−. Subsequently, step 2 was carried out by applying a positive potential for 10 s to form $-NH_2^{\bullet+}$. The process was repeated for a certain period to grow chains of pGA that were created by the combination of −COO− and ($-NH_2^{\bullet+}$) on the pencil lead surface. Fig. 1A illustrates a potentiostatic graph with the anodic and cathodic potentials of 2.0 and -1.0 V. The proposed mechanism of polymerisation of GA is illustrated in Fig. 1B.

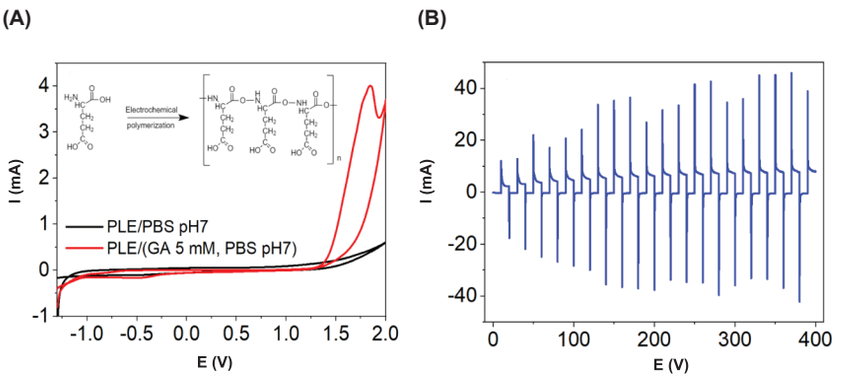

Fig. 1. (A) Cyclic voltammograms and (B) potentiostatic graphic of PLE in pGA solution and during the polymerisation reaction of pGA.

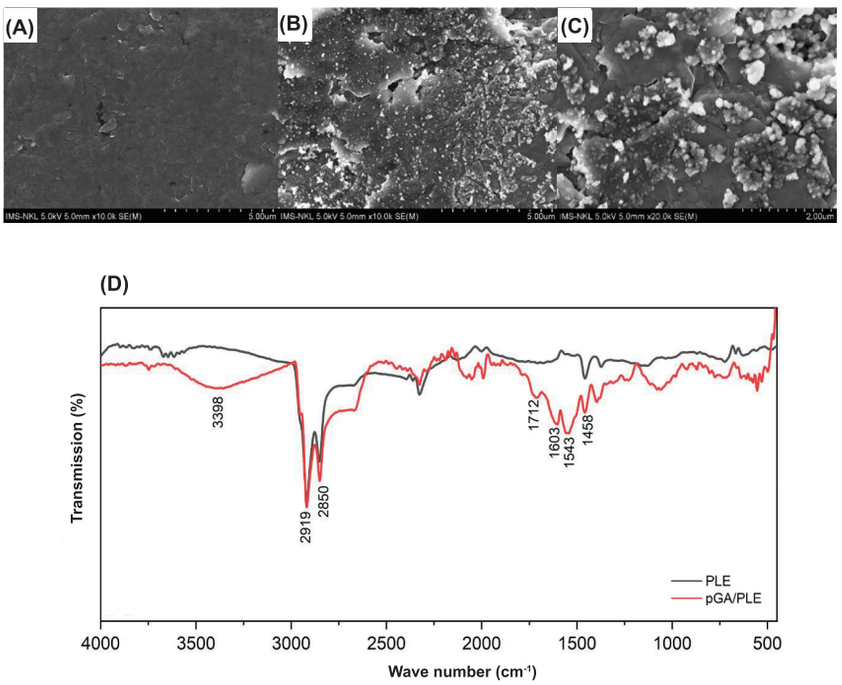

Fig. 2. SEM images of (A) PLE and (B, C) pGA/PLE at different magnifications, (D) ATR-FTIR spectra of PLE and pGA/PLE.

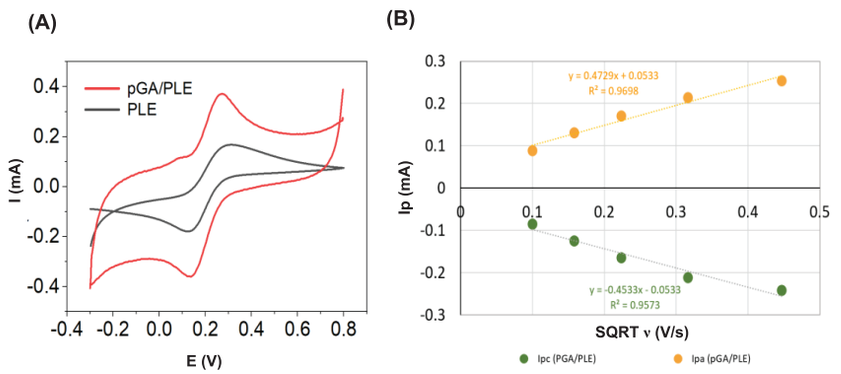

Fig. 3. Cyclic voltammograms of PLE (A) and pGA/PLE (B) in 5 mM $K_3Fe(CN)_6$ solution.

Figure 2 shows the SEM images of pGA/PLE on the electrode surface. As seen in Fig. 2A, the pencil lead electrode has a smooth surface. After modification, pGA clusters are present with a scattered distribution on the pencil lead substrate (Fig. 2B). At higher magnification as seen in Fig. 2C, pGA deposition is clearly identified with a cluster size of several hundred nanometres.

The presence of pGA on PLE can be confirmed by ATR-FTIR spectroscopy, as demonstrated in Fig. 2D. A comparison between the unmodified electrode and the pGA/PLE-modified electrode reveals distinct differences in the spectral peaks. Specifically, the pGA/PLE spectrum exhibits significant peaks at 3398 cm^{-1}, which can be attributed to the stretching vibration of both the N-H and O-H functional groups. Additionally, peaks at 1603, 1543 cm^{-1}, and 1712 cm^{-1}, which correspond to amide I, amide II, and C=O in the carboxylic group, respectively, are observed. These peaks are indicative of the presence of a pGA layer on the PLE electrode surface. Moreover, both the PLE and pGA/PLE electrodes show identical peaks at 2919, 2850, and 1458 cm^{-1}, which can be attributed to C-H stretching and C-C bending in the PLE composition. The obtained results agree with those of previous publications [26, 32-37].

3.2. Electrochemical properties of pGA/PLE

Electrochemical properties of pGA/PLE were examined by cyclic voltammetry. The measurements were performed by cyclic potential scanning from 0.8 to -0.2 V in PBS solution (pH 7) containing 5 mM $K_3Fe(CN)_6$ at different scanning rates. Fig. 3A reveals two clear peaks at 0.18 and 0.25 V, which correspond to the reduction of Fe^{3+} to Fe^{2+} and the oxidation of Fe^{2+} to Fe^{3+}, respectively. It is evident that the reduction peak on PGA/PLE is more symmetric and sharper than that of the pencil lead electrode. Also, the peak current on the modified electrode is higher than that of the unmodified one (Fig. 3A). These indicate that the PGA/PLE exhibited better electron transfer ability and a larger electrochemical active area than the unmodified electrode, which could improve the analytical signal.

Figure 3B illustrates a good linear relationship between peak current and the square root of the potential scanning rate in both oxidation and reduction directions with correlation coefficients of 0.9698 and 0.9573, respectively, indicating the electrochemical process was controlled by diffusion [38].

3.3. The response signal of ENR on the pGA/PLE

The electrochemical response of ENR on the prepared electrode was evaluated by using the SW-AdSV method in a 1 µM ENR solution. As can be seen in Fig. 4A, no peak appeared in the blank solution, while a peak at 0.8 V was clearly observed in the ENR solution. The peak is attributed to the oxidation of ENR on the electrode surface with a reaction mechanism proposed in Fig. 4B [39]. In addition, the result shows a much higher peak current on pGA/PLE than the signal on PLE (13.5 times higher). This increase could be explained by the improvement of ENR accumulation on pGA surface.

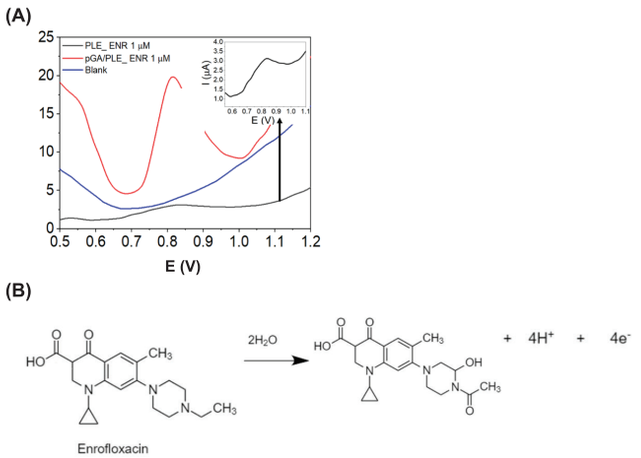

Fig. 4. (A) Square wave graph of PLE (black line) and pGA/PLE (red line) in 1 µM ENR solution; (B) The proposed mechanism of oxidation of ENR.

3.4. Optimisation of pGA/PLE polymerisation and pH of supporting electrolyte

ENR determination significantly depends on the preparation parameters and pH of the supporting electrolyte. This section details the influence of these parameters on the ENR signal.

Influence of polymerisation method on the ENR signal: In comparison with the pencil lead electrode modified with pGA by the cyclic voltammetry method, the ENR peak current on pGA/PLE produced by the potentiostatic method provided a higher ENR peak current (1.45 times higher) (Fig. 5A) and was three times faster. Therefore, to obtain sufficient ENR signal and to reduce preparation time, the potentiostatic method was chosen for electrode modification.

Influence of polymerisation cycle number on the ENR signal: The impact of cycle number in the polymerisation process on ENR signal was investigated by SWV in a PBS solution containing 1 µM ENR. As shown in Fig. 5B, when the cycle number changed from 1 to 20, the peak current significantly increased and reached its highest value at 20 cycles. The peak current gradually decreased over the range of cycles from 30 to 50. Therefore, the 20-cycle polymerisation process was chosen for the next experiment.

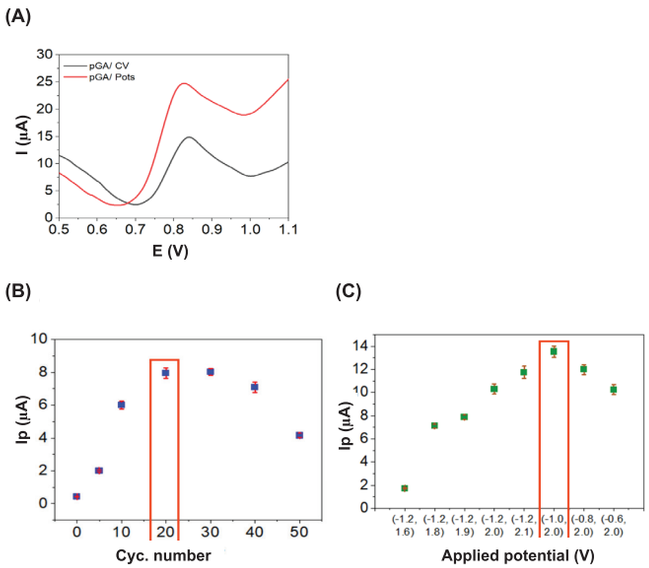

Fig. 5. (A) Square wave voltammograms in ENR solution of pGA/PLE fabricated by cyclic voltammetry and potentiostatic method; (B) Plot of ENR peak current vs cycle numbers; (C) Applied potentials in polymerisation.

Influence of applied polymerisation potential on the ENR signal: The applied potential used in the polymerisation step also plays a crucial role in the improvement of the ENR signal. Cathodic and anodic potential couples of -1.2 and 1.6 V, -1.2 and 1.8 V, -1.2 and 1.9 V, -1.2 and 2.0 V, -1.2 and 2.1 V, -1 and 2 V, -0.8 and 2 V, and -0.6 and 2 V were selected for the investigation. As demonstrated in Fig. 5C, among these potential couples, the highest ENR peak current was obtained when applying a potential couple of -1 and 2 V. These potential values were appropriate for polymerisation in that it supplied sufficient energy for the formation of the ions and free radicals. The decrease in peak current at more negative cathodic potentials and positive potentials could be because of the generation of hydrogen bubbles on the electrode surface, preventing polymer formation. Therefore, the polymerisation potential couple of -1 and 2 V was chosen for the following experiment.

The influence of pH on ENR signal: The pH value of the supporting electrolyte solution has a significant impact on the electrochemical oxidation of ENR. To determine an optimal pH value for ENR analysis, the oxidation signal was recorded in a PBS solution containing 1 µM ENR at different pH values (Fig. 6A). At pH of 4 and 5, relatively low peaks were obtained. Then, the peak currents increased with increasing pH value and the highest current was obtained at pH8. The peak current slightly decreased at pH9. Therefore, the PBS solution with pH8 was chosen as the optimal parameter for the analysis of ENR for the next experiments. Fig. 6B shows a linear relationship of pH value vs. peak potentials of ENR with the slope of the linear curve being 0.049, demonstrating that an equal number of electrons and protons were present in the ENR reaction. It is also observed in Fig. 6C that when pH was changed from 4 to 9, peak positions gradually moved to the negative direction. This result suggests that protons participated in the oxidation reaction of ENR.

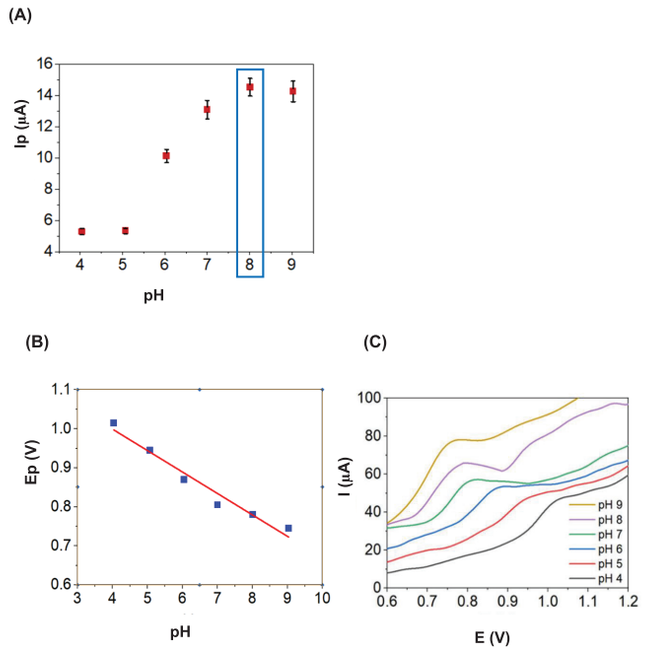

Fig. 6. Plots of ENR peak current vs pH (A) and ENR peak potential vs pH (B); square wave voltammograms of pGA/PLE in ENR solution at pH from 4 to 9 (C).

3.5. Calibration curve for ENR detection

After the optimisation of electrode preparation and analysis conditions, a calibration curve was established to evaluate the performance of ENR detection by SW-AdSV over a concentration range from 0.1 to 5 µM (Fig. 7). Within this concentration range, the peak current and ENR concentration are linearly correlated with the following regression equation: I_p (µA)=14.074 C_{ENR} (µM)-0.353. A correlation coefficient of 0.9988 was obtained. The reproducibility of the measurement was also investigated with an acceptable relative standard deviation of 4.3% (data not shown here). An LOD of 0.122 µM was obtained through the equation LOD=3σ/b; where σ and b are the standard deviation and the linear slope, respectively.

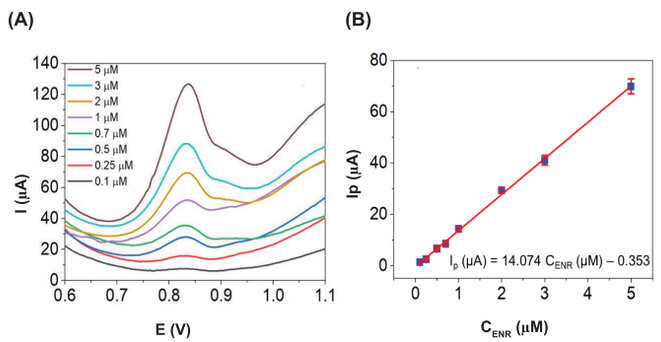

Fig. 7. (A) Square wave voltammograms of pGA/PLE in PBS solution containing ENR over a concentration range from 0.1 to 5 µM; (B) Calibration curve between peak current and concentration.

4. Conclusions

In this study, a novel sensor for ENR detection was successfully developed using polyglutamic-modified pencil lead graphite and a potentiostatic method. Optimal voltametric parameters, including applied cathodic (-1 V) and anodic (2 V) potentials were determined, and the synthesis time was set to 10 s for 20 cycles. The use of a PBS with pH8 was found to be a suitable medium for ENR detection. The sensor demonstrated acceptable reproducibility and a low detection limit of 0.12 µM for ENR. The results of this initial study suggest that the fabrication of the sensor is simple, low-cost, less time-consuming, and environmentally friendly. Thus, it has potential applications in ENR quantification.

CRediT author statement

Thi Hai Yen Pham: Idea and Conceptualisation, Research and Investigation, Revise and Editing, Supervision, Project administration; Thi Kim Ngan Nguyen: Research and Investigation; Thi Thu Hien Chu: Methodology, Writing; Thi Thu Ha Vu: Formal analysis, Writing - Review and Editing; Quoc Hung Le: Resources, Methodology.

ACKNOWLEDGEMENTS

This research is funded by Institute of Chemistry, Vietnam Academy of Science and Technology under grant number VHH.2022.08 and Vietnam National Foundation for Science and Technology Development (NAFOSTED) under grant number 104.06-2019.27.

COMPETING INTERESTS

The authors declare that there is no conflict of interest regarding the publication of this article.

REFERENCES

[1] B.D. Heins, D.V. Nydam, A.R. Woolums, et al. (2014), "Comparative efficacy of enrofloxacin and tulathromycin for treatment of preweaning respiratory disease in dairy heifers", *J. Dairy Sci.*, **97(1)**, pp.372-382, DOI: 10.3168/jds.2013-6696.

[2] E.J. Robb, C.M. Tucker, L. Corley, et al. (2007), "Efficacy of tulathromycin or enrofloxacin for initial treatment of naturally occurring bovine respiratory disease in feeder calves", *Vet. Ther.*, **8(2)**, pp.127-135.

[3] F. Yu, S. Yu, L. Yu, et al. (2014), "Determination of residual enrofloxacin in food samples by a sensitive method of chemiluminescence enzyme immunoassay", *Food Chem.*, **149**, pp.71-75, DOI: 10.1016/j.foodchem.2013.10.024.

[4] A.A. Gouda, A.S. Amin, R. El-Sheikh, et al. (2014), "Spectrophotometric determination of gemifloxacin mesylate, moxifloxacin hydrochloride, and enrofloxacin in pharmaceutical formulations using acid dyes", *Journal of Analytical Methods in Chemistry*, **2014**, DOI: 10.1155/2014/286379.

[5] B. Zhang, L. Lv, X. Ma, et al. (2022), "Au@ZnNi-MOF labeled electrochemical aptasensor for detection of enrofloxacin based on AuPt@h-CeO_2/MoS_2 and DNAzyme-driven DNA walker triple amplification signal strategy", *Biosensors and Bioelectronics*, **210**, DOI: 10.1016/j.bios.2022.114296.

[6] F.M. Salama, K.A. Attia, A.A. Abouserie, et al. (2018), "Potentiometric determination of Enrofloxacin using PVC and coated graphite sensors", *Glob. Drugs Therap.*, **3**, DOI: 10.15761/GDT.1000146.

[7] S. Wu, J. Mao, Y. Zhang, et al. (2023), "Sensitive electrochemical detection of enrofloxacin in eggs based on carboxylated multi-walled carbon nanotubes-reduced graphene oxide nanocomposites: Molecularlyimprintedrecognition versus direct electrocatalytic oxidation", *Food Chemistry*, **413**, DOI: 10.1016/j.foodchem.2023.135579.

[8] S.S. Khaloo, S. Mozaffari, A. Barekat, et al. (2015), "Fabrication of a modified electrode based on multi-walled carbon nanotubes decorated with iron oxide nanoparticles for the determination of enrofloxacin", *Micro & Nano Letters*, **10(10)**, pp.561-566, DOI: 10.1049/mnl.2015.0123.

[9] D. Wang, S. Jiang, Y. Liang, et al. (2022), "Selective detection of enrofloxacin in biological and environmental samples using a molecularly imprinted electrochemiluminescence sensor based on functionalized copper nanoclusters", *Talanta*, **236**, DOI: 10.1016/j.talanta.2021.122835.

[10] C. Canales, E. Peralta, M. Antilen (2019), "Electrochemical techniques to detect and quantify Enrofloxacin in presence of highly potential interferences: Assays in Chilean aqueous-soil matrices", *Journal of Electroanalytical Chemistry*, **832**, pp.329-335, DOI: 10.1016/j.jelechem.2018.10.064.

[11] M. Antilén, C. Valencia, E. Peralta, et al. (2017), "Enrofloxacin behavior in presence of soil extracted organic matter: An electrochemical approach", *Electrochimica Acta*, **244**, pp.104-111, DOI: 10.1016/j.electacta.2017.05.104.

[12] C. Bouki, D. Venieri, E. Diamadopoulos (2013), "Detection and fate of antibiotic resistant bacteria in wastewater treatment plants: A review", *Ecotoxicology and Environmental Safety*, **91**, pp.1-9, DOI: 10.1016/j.ecoenv.2013.01.016.

[13] X. Xu, L. Liu, Z. Jia, et al. (2015), "Determination of enrofloxacin and ciprofloxacin in foods of animal origin by capillary electrophoresis with field amplified sample stacking-sweeping technique", *Food Chemistry*, **176**, pp.219-225, DOI: 10.1016/j.foodchem.2014.12.054.

[14] A.O. Oyedeji, T.A.M. Msagati, A.B. Williams, et al. (2021), "Detection and quantification of multiclass antibiotic residues in poultry products using solid-phase extraction and high-performance liquid chromatography with diode array detection", *Heliyon*, **7(12)**, DOI: 10.1016/j.heliyon.2021.e08469.

[15] H. Tian (2011), "Determination of chloramphenicol, enrofloxacin and 29 pesticides residues in bovine milk by liquid chromatography-tandem mass spectrometry", *Chemosphere*, **83(3)**, pp.349-355, DOI: 10.1016/j.chemosphere.2010.12.016.

[16] J. Dai, Y. Wang, H. Lin, et al. (2023), "Residue screening and analysis of enrofloxacin and its metabolites in real aquatic products based on ultrahigh-performance liquid chromatography coupled with high resolution mass spectrometry", *Food Chemistry*, **404(B)**, DOI: 10.1016/j.foodchem.2022.134757.

[17] M.J.E. Souza, C.F. Bittencourt, L.M. Morsch (2002), "LC determination of enrofloxacin", *Journal of Pharmaceutical and Biomedical Analysis*, **28(6)**, pp.1195-1199, DOI: 10.1016/s0731-7085(01)00673-2.

[18] A.E. Radi (2010), "Application of electrochemical methods for analysis of fluoroquinolones antibacterial agents and fluoroquinolones-DNA interactions", *The Open Chemical and Biomedical Methods Journal*, **3**, pp.27-36, DOI: 10.2174/1875038901003010027.

[19] P. Wei, S. Wang, W. Wang, et al. (2022), "CoNi bimetallic metal-organic framework and gold nanoparticles-based aptamer electrochemical sensor for enrofloxacin detection", *Applied Surface Science*, **604**, DOI: 10.1016/j.apsusc.2022.154369.

[20] S. Han, X. Zhang, H. Sun, et al. (2022), "Electrochemical behavior and voltammetric determination of chloramphenicol and doxycycline using a glassy carbon electrode modified with single-walled carbon nanohorns", *Electroanalysis*, **34(4)**, pp.735-742, DOI: 10.1002/elan.202100354.

[21] E.M. Materón, A. Wong, T.A. Freitas, et al. (2021), "A sensitive electrochemical detection of metronidazole in synthetic serum and urine samples using low-cost screen-printed electrodes modified with reduced graphene oxide and C60", *Journal of Pharmaceutical Analysis*, **11(5)**, pp.646-652, DOI: 10.1016/j.jpha.2021.03.004.

[22] R. Nehru, C.D. Dong, C.W. Chen (2021), "Cobalt-doped Fe_3O_4 nanospheres deposited on graphene oxide as electrode materials for electrochemical sensing of the antibiotic drug", *ACS Applied Nano Materials*, **4(7)**, pp.6768-6777, DOI: 10.1021/acsanm.1c00826.

[23] T.S.K. Sharma, K.Y. Hwa (2021), "Facile synthesis of Ag/AgVO(3)/N-rGO hybrid nanocomposites for electrochemical detection of levofloxacin for complex biological samples using screen-printed carbon paste electrodes", *Inorg. Chem.*, **60(9)**, pp.6585-6599, DOI: 10.1021/acs.inorgchem.1c00389.

[24] A. Feizollahi, A.A. Rafati, P. Assari, et al. (2021), "Development of an electrochemical sensor for the determination of antibiotic sulfamethazine in cow milk using graphene oxide decorated with Cu-Ag core-shell nanoparticles", *Analytical Methods*, **13(7)**, pp.910-917, DOI: 10.1039/D0AY02261F.

[25] A.M. Golkarieh, N. Nasirizadeh, R. Jahanmardi (2021), "Fabrication of an electrochemical sensor with Au nanorods-graphene oxide hybrid nanocomposites for in situ measurement of cloxacillin", *Mater. Sci. Eng. C Mater. Biol. Appl.*, **118**, DOI: 10.1016/j.msec.2020.111317.

[26] Y. Lin, K. Liu, C. Liu, et al. (2014), "Electrochemical sensing of bisphenol A based on polyglutamic acid/amino-functionalised carbon nanotubes nanocomposite", *Electrochimica Acta*, **133**, pp.492-500, DOI: 10.1016/j.electacta.2014.04.095.

[27] X. Liu, L. Luo, Y. Ding, et al. (2011), "Poly-glutamic acid modified carbon nanotube-doped carbon paste electrode for sensitive detection of L-tryptophan", *Bioelectrochemistry*, **82(1)**, pp.38-45, DOI: 10.1016/j.bioelechem.2011.05.001.

[28] Y. Zhang, L. Luo, Y. Ding, et al. (2010), "A highly sensitive method for determination of paracetamol by adsorptive stripping voltammetry using a carbon paste electrode modified with nanogold and glutamic acid", *Microchimica Acta*, **171(1)**, pp.133-138, DOI: 10.1007/s00604-010-0422-1.

[29] J. Thangphatthanarungruang, C. Chotsuwan, W. Siangproh (2023), "A novel and easy-to-construct polymeric l-glutamic acid-modified sensor for urinary 1-hydroxypyrene detection: Human biomonitoring of polycyclic aromatic hydrocarbons exposure", *Talanta*, **253**, DOI: 10.1016/j.talanta.2022.123929.

[30] C. Chen, X. Lv, W. Lei, et al. (2019), "Amoxicillin on polyglutamic acid composite three-dimensional graphene modified electrode: Reaction mechanism of amoxicillin insights by computational simulations", *Analytica Chimica Acta*, **1073**, pp.22-29, DOI: 10.1016/j.aca.2019.04.052.

[31] J.J. Feminus, R. Manikandan, S.S. Narayanan, et al. (2019), "Determination of gallic acid using poly(glutamic acid): Graphene modified electrode", *Journal of Chemical Sciences*, **131(2)**, DOI: 10.1007/s12039-018-1587-0.

[32] O. Suys, A. Derenne, E. Goormaghtigh (2022), "ATR-FTIR biosensors for antibody detection and analysis", *Int. J. Mol. Sci.*, **23(19)**, DOI: 10.3390/ijms231911895.

[33] O. Gördük (2021), "Poly(glutamic acid) modified pencil graphite electrode for voltammetric determination of bisphenol A", *Journal of the Turkish Chemical Society Section A: Chemistry*, **8(1)**, pp.173-186, DOI: 10.18596/jotcsa.728165.

[34] J. Kumirska, M. Czerwicka, Z. Kaczyński, et al. (2010), "Application of spectroscopic methods for structural analysis of chitin and chitosan", *Marine Drugs*, **8(5)**, pp.1567-1636, DOI: 10.3390/md8051567.

[35] E.H. Alsharaeh, A.A. Othman, M.A. Aldosari (2014), "Microwave irradiation effect on the dispersion and thermal stability of RGO nanosheets within a polystyrene matrix", *Materials (Basel)*, **7(7)**, pp.5212-5224, DOI: 10.3390/ma7075212.

[36] B. Sadhasivam, S. Muthusamy (2016), "Synthesis and characterization of optically active polyimides and their octa(aminophenyl) silsesquioxane nanocomposites", *Sage Journals*, **28(5)**, pp.547-561, DOI: 10.1177/0954008315591021.

[37] S. Karamikamkar, M. Fashandi, H.E. Naguib, et al. (2020), "In situ interface design in graphene-embedded polymeric silica aerogel with organic/inorganic hybridization", *ACS Applied Materials & Interfaces*, **12(23)**, pp.26635-26648, DOI: 10.1021/acsami.0c04531.

[38] T.H.Y. Pham, T.T. Mai, H.A. Nguyen, et al. (2021), "Voltammetric determination of amoxicillin using a reduced graphite oxide nanosheet electrode", *Journal of Analytical Methods in Chemistry*, **2021**, DOI: 10.1155/2021/8823452.

[39] M.P. Deepak, G.P. Mamatha (2016), "Simultaneous determination of ciprofloxacin hydrochloride and enrofloxacin at poly (furosemide) modified carbon paste electrode by cyclic voltammetry", *Journal of Chemical and Pharmaceutical Research*, **8(6)**, pp.387-398.